SUPPORTING INFORMATION

SI Materials and Methods

Construction of amiRNA Lines

Artificial miRNAs targeting *AP3* and *PI* mRNAs were designed using the web-based design tools WMD (http://wmd.weigelworld.org) and WMD2 (http://wmd2.weigelworld.org), respectively. The backbone of the plasmid pRS300 was used as a template for a PCR-based mutagenesis as described previously (1). In total, two amiRNAs targeting *AP3* and ten targeting *PI* were designed (see Table S1). The resulting amiRNAs were inserted into the shuttle vector pBJ36 (2), either containing a 35S Cauliflower Mosaic Virus promoter (3) or the pAlcA ethanol receptor responsive promoter from *Aspergillus nidulans* (4, 5) using *Eco*RI/*Bam*HI restriction sites. The amiRNAs under the control of the 35S promoter were then inserted into the plant transformation vector pML-BART (2) using *Not*I restriction sites. To generate the constructs required to obtain ethanol-inducible amiRNA lines, the amiRNA sequences under the control of the AlcA promoter were inserted into a pML-BART derivative containing the AlcR-receptor driven by the 35S promoter using *Not*I restriction sites. These constructs were used to transform L-*er* wild-type plants. The most suitable 35S:AlcR/pAlcA:AP3-amiRNA transgenic line was crossed with the previously described 35S:AP1-GR *ap1-1 cal-1* floral induction system (6). Plants homozygous for all transgenes and mutations were subsequently isolated.

Construction of AP3-GFP and PI-GFP Lines for ChIP

To generate the pAP3:AP3-GFP translational fusion, a genomic fragment containing the *AP3* locus was PCR amplified from L-*er* genomic DNA using primers oSW-140/146 (see Table S4 for primers used) and digested using *Sma*I. The digested PCR fragment was then subcloned into pBJ36-mGFP5 treated with the same restriction enzyme. To generate the pPI:PI-GFP translational fusion, a genomic fragment containing the *PI* locus was PCR amplified from genomic DNA from L-*er* plants using primers oSW-138/139, and digested using *Pst*I/*Xho*I. The digested PCR fragment was then subcloned into pBJ36-mGFP5 using *Pst*I/*Xho*I sites. Both the pAP3:AP3-GFP and pPI:PI-GFP translational fusions were then inserted into the plant transformation vector pML-BART (2) using *Not*I restriction sites. Plant populations segregating the *ap3-3* and *pi-1* alleles, respectively, were transformed using these pML-BART derivatives. Selected transgenic lines that restored *AP3* and *PI* function, respectively, were crossed into the previously described 35S:AP1-GR *ap1-1 cal-1* floral induction system (6). Plants homozygous for all transgenes and mutations were isolated in subsequent generations.

Plant Transformation

Agrobacterium-mediated plant transformation (using strain C58 pGV2260 (7)) was carried out using the floral-dip method (8). T1 transgenic seedlings transformed with pML-BART derivatives were identified by spraying seedlings with 200 μg/mL ammonium-glufosinate. For plants of accession Landsberg *erecta* (L-*er*), transformation was performed by applying a vacuum of 500 mbar for 5 min while inflorescences were submerged in the transformation solution.

Induction of Flower Development

For all experiments, we used ~4 week-old 35S:AP1-GR *ap1-1 cal-1* plants. Flower development was induced as described (9), using a solution containing 10 μM dexamethasone (Sigma-Aldrich), 0.01% (v/v) ethanol and 0.015% (v/v) Silwet L-77 (De Sangosse).

Induction of amiRNA Expression Using Ethanol Vapor

Plants were transferred into trays that can be covered by plastic lids (18 cm x 32 cm x 50 cm). Two 50 mL tubes containing 10 mL of 100% ethanol each were placed near the plants before the lid was closed. For the mock treatments, ethanol was replaced with water.

Phenotypic Series of *AP3* and *PI* Perturbation

Plants were treated with a single 24 h pulse of ethanol vapor and flowers were observed every day and photographed at anthesis. Floral phenotypes were assessed with an Olympus SZX7 zoom stereomicroscope. Epidermal surface imprints were generated as described (10). Imaging was performed using an Olympus BX61 fluorescence microscope with differential interference contrast optics.

Epifluorescence Microscopy and Confocal Imaging

GFP fluorescence was visualized with an Olympus BX61 fluorescence microscope with

excitation wavelengths of 460/480 nm and emission wavelengths of 495-540 nm. A Zeiss LSM 510 confocal microscope equipped with a 40X C-Apochromat Lens was used to visualize the AP3-GFP fusion protein. For this purpose, older flower buds were removed from freshly harvested inflorescences of plants that had been grown at 16ºC for two days. The plasma membranes were stained using 10 µL of a ~330 µg/mL FM4-64 solution. After removing the excess dye, GFP was excited at 488 nm, the filter range 505-550 nm was defined as green (GFP) signal and 585 nm was defined as red (FM4-64).

Detection of GFP-Containing Fusion Proteins by Western Blotting

Inflorescence tissue of transgenic plant lines was taken 4 d after dexamethasone treatment. Nuclear extracts from plants were prepared from these tissues as described previously (11). Proteins were separated on a 10% SDS-PAGE gel, followed by transfer to a PVDF membrane. GFP was detected using a rabbit antibody (Ab290, Abcam) diluted 4,000-fold in PBS-T [1 × PBS with 0.05% (v/v) Tween 20] supplemented with 5% (w/v) milk.

PCR Genotyping of Mutant Alleles and T-DNA Insertions

Genomic DNA was extracted from selected plants as described (12) and used for PCR genotyping. Genotyping of *pi-1*, *ap3-3* and *ap3-1* was performed as described (13-15). The presence of the T-DNA insertion in *rbe-101* was confirmed using primers oSW-722 and SAIL_LB (see Table S4 for primers used), whereas the absence of the T-DNA was confirmed using primers oSW-721 and oSW-722. The presence of the *rbe-102* T-DNA insertion was confirmed using primers oSW-718 and SALK_LB, whereas the absence of the

rbe-102 T-DNA insertion was confirmed using primers oSW-717 and oSW-718. Furthermore, the genomic sequences flanking the left border of the T-DNA insertions were determined by Sanger sequencing. The presence of the T-DNA insertion in *ufo-101* was verified using primers KH141 and SALK_LB2, whereas the absence of T-DNA was confirmed using oligonucleotides KH141 and KH171. Plant homozygous for the transposon in *ufo-102* were isolated using the following sets of primers: KH171 and KH144 (presence of the transposon), and KH171 and KH141 (genome-specific primers). The genomic sequences flanking the right borders of the T-DNA and transposon insertions were determined by Sanger sequencing.

In situ Hybridization

Non-radioactive *in situ* hybridizations were performed as previously described (16). Part of the *CRC* cDNA was amplified by PCR using primers oSW-689 and oSW-690. The PCR product was ligated into pGEM-T Easy (Promega) and the resulting vector was sequenced to determine the orientation of the insert.

RNA Preparation

Total RNA was isolated from tissue samples using the Plant Total RNA kit (Sigma-Aldrich). Quality of selected RNA samples was evaluated using a Bioanalyzer and a RNA Nano 6000 kit (Agilent).

Tissue Collection for Microarray Experiments

At least four biologically independent sets of samples were generated for each experiment and time point. For all experiments, we used ~4 week-old plants. We collected inflorescence tissue from plants before applying the dexamethasone-containing solution (0 d time-point), as well as 2.5 and 5 d after dexamethasone treatment. The plants used were the offspring from a cross between plants that were heterozygous for the *ap3-3* or *pi-1* mutant alleles (in the floral induction system) and plants that were homozygous for *ap3-3* or *pi-1* (also in the floral induction system). Inflorescence tissue from ~45 plants per time-point was collected individually. After tissue collection, the phenotype of the flowers stemming from the secondary inflorescences was examined to infer the genotype of the plant. When the results of this phenotyping approach were inconclusive, PCR-based genotyping was performed as described above. The tissue from ~20 individual plants identified as being homozygous for *ap3-3* or *pi-1* was pooled for each time-point taken. In addition, tissue from plants that formed wild-type flowers (*i.e*. were heterozygous for *ap3-3* or *pi-1*) was also combined, resulting in the control samples for the different time-points taken.

For the temperature-shift experiments, three biologically independent sets of samples were generated. We collected inflorescence tissue from plants that were homozygous for the *ap3-1* allele in the floral induction system 2, 3, 5 and 6 d after dexamethasone treatment. Plants were grown at 16ºC and inflorescence tissue was collected before transferring to a non-permissive temperature (days 2 and 5), and after 24 h at 27ºC (days 3 and 6). As a control, 35S:AP1-GR *ap1-1 cal-1* plants that contained the wild-type allele of *AP3* were treated in an identical manner. The need to use different growth and treatment conditions

for the *ap3-3* and *pi-1* null mutants on the one hand and the temperature-sensitive allele *ap3-1* on the other resulted in slight differences in the progression of flower development, so that a given stage was reached at different times after floral induction. To compensate for this, we collected flowers of similar stages at different time-points so that the 2.5 and 5 d time-points of the *ap3-3* and *pi-1* experiments are roughly equivalent to the 3 and 6 d time-point of the *ap3-1* experiment.

Microarray data from whole inflorescence tissue was generated from three biologically independent sets of samples. Plants that were homozygous for the *ap3-1* allele were grown at 16ºC before being shifted to 27ºC for 24 h. Older flower buds were removed from inflorescences, so that flowers up to ~stage 10 were collected. As a control, L-*er* wild-type plants were treated in an identical manner.

Microarray Experiments and Data Analysis

Custom microarrays manufactured by Agilent (Agilent Technologies, Santa Clara, CA) were designed as previously described (11). The dyes used for labeling RNA from plants of a given genotype were switched for the replicate experiments to reduce dye-related artifacts. Dye-labelled RNA from mutant and wild-type samples for each time-point and biological replicate were co-hybridized.

Probes on the Agilent array (their design was based on the *Arabidopsis* genome release version 8) were re-annotated to match version 10 as outlined below. Low-level data processing was performed using functionality provided by *limma* Version 2.14.0 (17). Agilent median signals and background were read into *R* and background correc-

tion was performed using the *backgroundCorrect*-function (18) with maximum likelihood estimation of the background (17) and an offset of 50. Between-channel normalization was performed using loess-normalization, between-array normalization using quantile normalization (19). Signals of probes targeting transcripts from the same locus were averaged using the *avereps*-function provided in the *limma* package. Non-specific filtering was performed using the *genefilter* package Version 1.36.0, based on a signal cut-off determined by the median signal from negative probe signals, so that only those probes with higher signals in at least three arrays were retained. Principal component analyses were performed using the *prcomp*-function in *R*.

Base-level annotations were retrieved from the Bioconductor homepage, (package *arabidopsis.db0* Version 2.6.4) and an annotation package for the custom-made 44K Agilent array was generated using *AnnotationDbi* package (Version 1.16.10). Gene ontology terms contained within the "biological process" class were used for further analyses, and terms with less than nine associated genes were removed. In order to reduce the number of statistical tests performed for GO analyses, redundancy between closely related terms was eliminated as follows: parent terms were removed if they had more than 90% percent gene-association overlaps with the combination of their daughter terms.

Pfam- and Gene family information was retrieved from the TAIR homepage (files 'gene_families_sep_29_09_update.txt' and 'TAIR10_all.domains'). *Arabidopsis* Gene Identifiers (AGIs) for the gene family record of the "B3 transcription factor family" were missing and therefore manually updated according to the previously proposed

naming scheme (20). Only families with nine or more associated genes were included in the analysis. Redundancy among protein families were removed by searching for protein families that had more than 90% overlaps in gene-associations with another family, and removing the smaller family from further analyses. The same procedure was used to remove redundant gene families.

Testing for differential gene expression was performed using linear models (21) as described in the *limma* user guide. Our data analysis mainly focused on functional groups of genes (*e.g*. GO terms, gene/protein families) over-represented within lists of potentially misexpressed genes. Therefore, the multiple testing adjustments were performed at the level of enrichment tests rather than at the level of selection of "differentially expressed" genes. Our gene selection strategy was based on declaring a gene as "differentially expressed" at a p-value< 0.01. GO enrichment analyses and protein/gene family enrichment analyses were performed using a two-sided Fisher's Exact Test implemented in *R*. Adjustments for multiple testing were performed using the *p.adjust* function in *R*, using Benjamini and Hochberg (BH) adjustments (22).

To test for coordinated changes of gene expression within selected functional groups, gene set enrichment analysis was performed using the *mroast* function as implemented in the *limma* package (23) with 10,000 rotations and "msq" summary set statistic that is sensitive to smaller proportions of differentially expressed genes within gene sets. Heat-maps were generated using the *gplots* package version 2.10.1.

Microarray Probe Re-Annotation

Probes on the Agilent array (their design was based on the *Arabidopsis* genome release version 8) were re-annotated to match the *Arabidopsis* genome release version 10. To this end, the standalone BLAST executable function *blastall* Version 2.2.24 (downloadable from ftp://ftp.ncbi.nih.gov/blast/executables/) (24) was used to map all probes to the latest cDNA definitions (file TAIR10_cdna_20101214 from www.arabidopsis.org); if a probe had one hit to transcript(s) from a single locus with two or less mismatches or no more than one gap-extension it was assigned the corresponding locus. Negative probes (*i.e.* whose sequences do not show similarities to any cDNA sequences, transposable elements or genomic sequences) were identified as follows: if no cDNA hit was found, the probe sequence was compared by BLAST against the transposable elements (TE) sequences (file 'TAIR9_TE.fasta'). If the BLAST search did not result in any hits (with two or less mismatches or no more than one gap-extension), it was further compared against genomic sequences (file 'TAIR10_bac_con_20101028'). If a probe had no hits with less than four mismatches or three gap-extensions, it was labeled as "negative probe" and used later to determine an empirical signal-cutoff for intensity-based filtering. All other probes were removed from the analysis.

qRT-PCR Experiments

cDNA synthesis was performed using total RNA preparations, oligo-dT primers and the RevertAid H Minus M-MuLV reverse transcriptase (Fermentas). Relative transcript abundance of selected genes was determined using the Roche LightCycler 480 system and the LC480 SYBR Green I Master kit (Roche Applied Sciences). See Table S5 for primers used. Measurements were taken for three to four biologically independent sets of samples. In ad-

dition, all PCR reactions were performed twice for each cDNA (technical duplicates). LightCycler melting curves were obtained for the reactions, revealing single peak melting curves for all amplification products. The amplification data were analyzed using the second derivative maximum method, and resulting Cp values were converted into relative expression values using the comparative Ct method (25). Two reference genes ('REF2' and 'REF3') (26) were used to normalize the data. Their Cp values were averaged for each sample.

Chromatin Immunoprecipitation

Chromatin preparation was performed using a modified version of a previously described protocol (27). The modifications employed for this study are outlined below. Inflorescences of approximately 4 week-old 35S:AP1-GR pAP3:AP3-GFP *ap1-1 cal-1 ap3-3*, 35S:AP1-GR pPI:PI-GFP *ap1-1 cal-1 pi-1* and 35S:AP1-GR *ap1-1 cal-1* plants were treated with a dexamethasone-containing solution and inflorescence material from these plants (~500-750 μL) was collected 4 d after the treatment and fixed for 60 min (the vacuum was released and reapplied every 15 min) in 1% (v/v) formaldehyde in MC buffer (10 mM sodium phosphate pH 7.0, 50 mM NaCl, 0.1 M sucrose). The formaldehyde was quenched using 0.125 M glycine under vacuum (800 mbar) for further 5 min, followed by three washes with MC buffer. The tissue was then quick frozen in liquid nitrogen and ground in 250 μL of M1 buffer (10 mM sodium phosphate pH 7.0, 0.1 M NaCl, 1 M 2-methyl 2,4-pentanediol, 10 mM β-mercaptoethanol, 1x Complete Protease Inhibitor Cocktail (Roche)) until homogenous. The suspension was then diluted to a final volume of 1.5 mL using M1 buffer. The

ground tissue was filtered twice through a layer of miracloth (25 μM, Merck). The filtered extract was then centrifuged for 5 min at 7,700 *g* and 4ºC to pellet the nuclei. The nuclei pellet was resuspended in 0.9 mL M2 buffer (M1 buffer with 10 mM $MgCl_2$, 0.5% Triton X-100), followed by centrifugation for 1 min at 7,700 *g* and 4ºC. This step was repeated twice. Then, the pellet was resuspended in 0.9 mL M3 buffer (M1 without 2-methyl 2,4-pentanediol), followed by centrifugation for 5 min at 2,000 *g* at 4ºC. The nucleus pellet was finally resuspended in 0.2 mL lysis buffer (50 mM Tris-HCl pH 8.1, 10 mM EDTA, 1% SDS, 1xCPIC) and incubated for 10 min on ice in order to lyse the nuclei. After incubation, the nuclei extract was diluted with 0.8 mL ChIP dilution buffer (16.7 mM Tris-HCl pH 8.1, 167 mM NaCl, 1.2 mM EDTA, 1.1% Triton X-100, 0.01% SDS, 1x CPIC). Chromatin was prepared by sonicating the resuspended and lysed nuclear extract in a Diagenode Bioruptor at 4ºC. Twelve cycles of 30 s sonication and 30 s cooling were applied (at "high" sonication intensity settings). DNA fragments obtained from sonicated chromatin ranged on average between 350 and 750 bp in size. The sonicated chromatin was centrifuged for 12 min at full speed and 4ºC to pellet cellular debris; the supernatant was frozen and stored at -80ºC until further use. The chromatin immunoprecipitation experiments and library preparation were performed as described (28). Chromatin samples were prepared for preclearing by adding IP buffer (50 mM HEPES pH 7.5, 150 mM NaCl, 5 mM $MgCl_2$, 10 μM $ZnSO_4$, 1% Triton X-100 and 0.05% SDS) to a total volume of 2 mL. The chromatin was then centrifuged 10 min at 18,600 *g* and 4°C to remove any precipitate. Instead of preclearing using pre-immune serum, samples were incubated with 30 μL (settled resin) of Protein A Sepharose 4 Fast Flow beads (GE Healthcare) for 90 min at 4°C and then spun for 1 min at

18,600 *g* and 4ºC. For ChIP, 4 μL of a GFP-specific antibody (Ab290, Abcam) was added per 2 mL of prepared chromatin.

Next-Generation Sequencing and Data Analysis

Two biologically independent samples were used to identify PI binding sites, whereas for AP3 and for the background control, one sample was used, respectively. ChIP-Seq libraries were clustered and sequenced using v5 Single Read Cluster Kits and v5 SBS kits (Illumina Inc, San Diego, Ca, USA). Sequence data (42 cycles) was generated on an Illumina GAIIx machine running data collection SCS2.9/RTA1.9 software. Short sequence read datasets from ChIP-Seq experiments for AP1 (11), SEP3 (29), LFY (30) and AP2 (31) were downloaded from the NCBI SRA database (www.ncbi.nlm.nih.gov/sra) and processed. *Arabidopsis* genomic sequences were downloaded from TAIR (www.arabidopsis.org; files 'TAIR10_chr1.fas' - 'TAIR10_chr5.fas'). Short read alignments were performed using the *SOAP2* software (32) with default settings. Data were read into *R* using the *CSAR* package (33), and functionality provided by various Bioconductor packages (including the *IRanges* v1.12.5 and *GenomicRanges* v1.6.4 packages) was used for data handling operations. Pattern matching was performed using the *Biostrings* package (version 2.22.0). Genomic sequences for use within *R* were retrieved from *BSgenome.Athaliana.TAIR.TAIR9* (Version 1.3.18).

Peak calling was performed using the *CSAR* package that included a normalization and a test based on the Poisson distribution (33), and enriched regions were identified at a False Discovery Rate (FDR)<0.001 (with five rounds of permutations for each

dataset, resulting in >600,000 permutations). Default parameters were used. Only peak regions with stretches of >50 bp were retained. In order to validate detected peak regions, the peak calling was repeated using independent short-read aligner and peak calling tools before merging biological replicates as described below.

Peaks were associated with genes located in the vicinity using *CSAR* functionality, whereby a peak had to reside in a genomic region ranging from 3 kb upstream of a gene's transcriptional start position to 1 kb downstream of its transcriptional end position. Gene range definitions were downloaded from TAIR (file TAIR10_GFF3_genes.gff). GO term enrichments were performed as described for the microarray analyses, by using GO mappings provided in the *org.At.tair.db* data package (version 2.6.4) downloaded from the Bioconductor homepage. Visualization of genomic regions was performed using the *GenomeGraphs* package Version 1.14.0 (34).

Alternative Peak Calling Method and Merging of Biological Replicates

In order to validate peak regions detected by the CSAR software, the peak calling was repeated using independent short-read aligner and peak calling tools as follows: short-reads were aligned to the reference genome using *BWA* version 0.6.1 (35), aligned reads were sorted and duplicated reads removed using *samtools* (36), and peak calling was performed using *MACS* Version 1.4.1 with default parameters (37). Peaks as determined by the *CSAR* software were then retained only if they had any overlap with peaks determined by the *MACS* software. In order to merge biological replicates from the PI-GFP ChIP-Seq experiments, peak definitions determined for PI-GFP replicate 2 were retained only if they

showed any overlap with the PI-GFP replicate 1.

Publicly Available ChIP-Seq Data

Short sequence read datasets from ChIP-Seq experiments for AP1 (11), SEP3 (29), LFY (30) and AP2 (31) were downloaded from the NCBI SRA database (www.ncbi.nlm.nih.gov/sra) and sequence information from the sra-files dumped into fastq-files using the *sratoolkit* (Version 2.0.1) software as described in the manual at www.ncbi.nlm.nih.gov/books/NBK47540. In some cases, the read numbers or qualities of replicates in these reference datasets were found to vary slightly: from the SEP3 dataset, only replicate 1 was used; from the LFY dataset, only replicate 2 was used and the two control replicates were merged to obtain a similar number of reads in control and sample. Quality control of the sequenced libraries was performed using the *FastQC* software (www.bioinformatics.bbsrc.ac.uk/projects/fastqc/).

Calculation of Relative Enrichment Scores of ChIP-Seq Data

Determination of per-base enrichment scores for the heat-maps shown in Fig. 5D and Fig. S8C was performed using custom *R* scripts. For this, the per-base enrichment scores based on a Poisson distribution were calculated by the *CSAR* package. Subsequently, the enrichment score cut-off for peak detection, at a FDR of 0.001, was determined using five rounds of permutations. This score was used as a normalization factor, and per-base enrichment scores were divided by this normalization factor (so that a normalized enrichment score of 1 denotes the enrichment score at an FDR of 0.001 and a normalized score of 2 denotes

twice this score, etc.). Normalized scores higher than 5 were truncated to the value of 5 for better visualization.

Detection of Motifs Present at Putative AP3/PI Binding Sites

For the detection of motifs at putative binding sites of PI/AP3, peaks with overlap between PI and AP3 experiments were determined, and peak definitions from the PI experiment were retained for these peaks. 400 bp core sequences centered around peak locations were submitted to the browser-based *MEME-ChIP* analysis suite (http://meme.sdsc.edu/meme/) (38). Sequence patterns from the DREME-software output (39) were matched back onto the reference genome using the *matchPattern*-function from the *Biostrings* package, position weight matrices from the MEME-software output (40) were matched using the *matchPWM*-function and a minimum score of 80%. Peaks associated with up-regulated genes were defined as any peaks residing within -3 kb upstream to +1 kb downstream of a gene that was significantly up-regulated at any time point in the *ap3-3* or *pi-1* null mutant experiments but not significantly down-regulated at any other time-point or experiment (a single peak can be associated with multiple genes and conversely, multiple peaks can be associated with a single gene). Peaks associated with down-regulated genes were defined accordingly.

ChIP-qPCR Experiments

Tissue was collected from ~4 week-old 35S:AP1-GR pPI:PI-GFP *ap1-1 cal-1 pi-1* and 35S:AP1-GR *ap1-1 cal-1* plants 4 d after dexamethasone treatment. ChIP was carried out, as described above, using 2 μL of a GFP antibody (A6455 from Invitrogen). Relative DNA

abundance of selected genomic regions was then determined using the Roche LightCycler 480 system and the LC480 SYBR Green I Master kit (Roche Applied Sciences). See Table S6 for primers used. Measurements were taken for three biologically independent sets of samples. LightCycler melting curves were obtained for the reactions, revealing single peak melting curves for all amplification products. The amplification data were analyzed using the second derivative maximum method, and resulting Cp values were converted into relative enrichment values using the comparative Ct method where 'Input' DNA was used to normalise the data (25). The 'Input' DNA was a sample of the chromatin available for precipitation that was extracted prior to the addition of antibody to account for differences in the solubility of different genomic regions, the shearing of DNA and amplification. Four genomic reference regions ('ACT7', 'REF1' (11), 'Mu' (41) and 'BRI1 negative region') were used to normalize the data. Their Cp values were averaged for each sample.

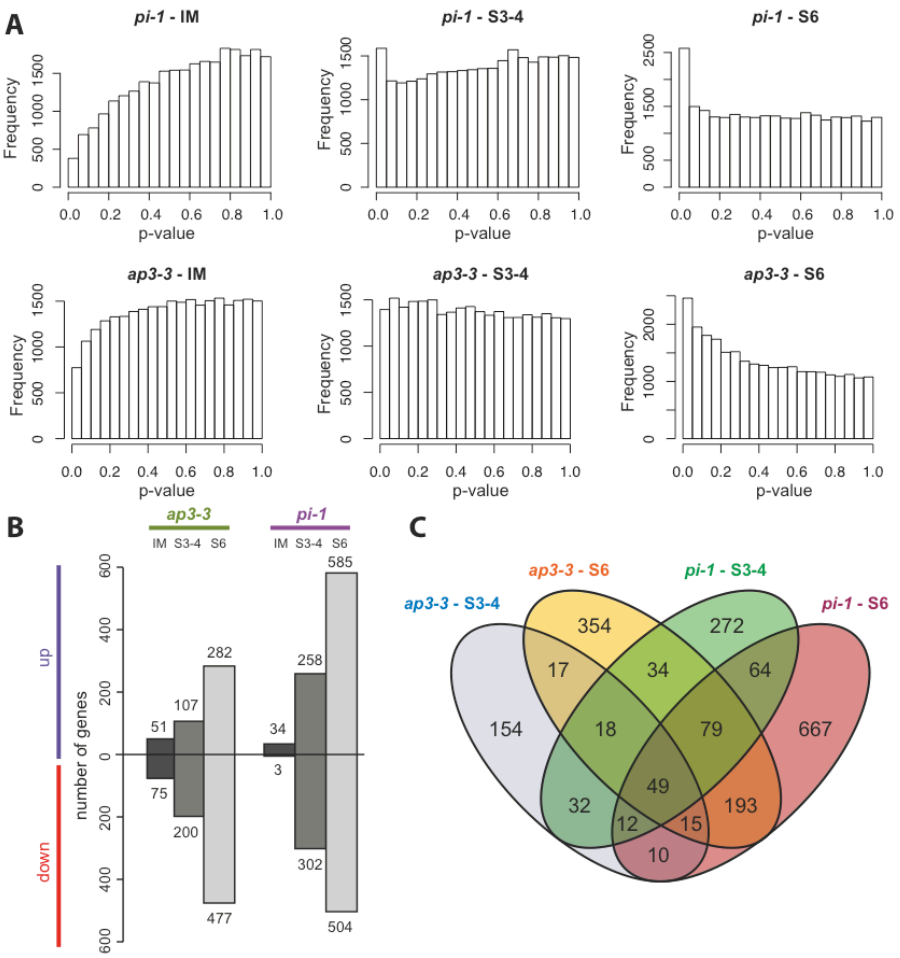

Fig. S1. Overview of microarray data from null-mutant experiments. (**A**) *P*-value histograms indicating the distribution of *p*-values for genes tested for differential expression in the microarray analysis of *ap3-3* and *pi-1* mutant flowers of different stages (S) (inflorescence-like meristems (IM), stage 3-4 and stage 6, corresponding to 0, 2.5 and 5 d after induction of flower formation). (**B**) Differentially expressed genes ($p<0.01$) identified in the *ap3-3* and *pi-1* experiments. The number of up and downregulated genes is indicated for each dataset. (**C**) Four-way Venn diagram depicting the overlap between the differentially expressed genes identified in *ap3-3* and *pi-1* mutant flowers of stages 3-4 and 6, respectively.

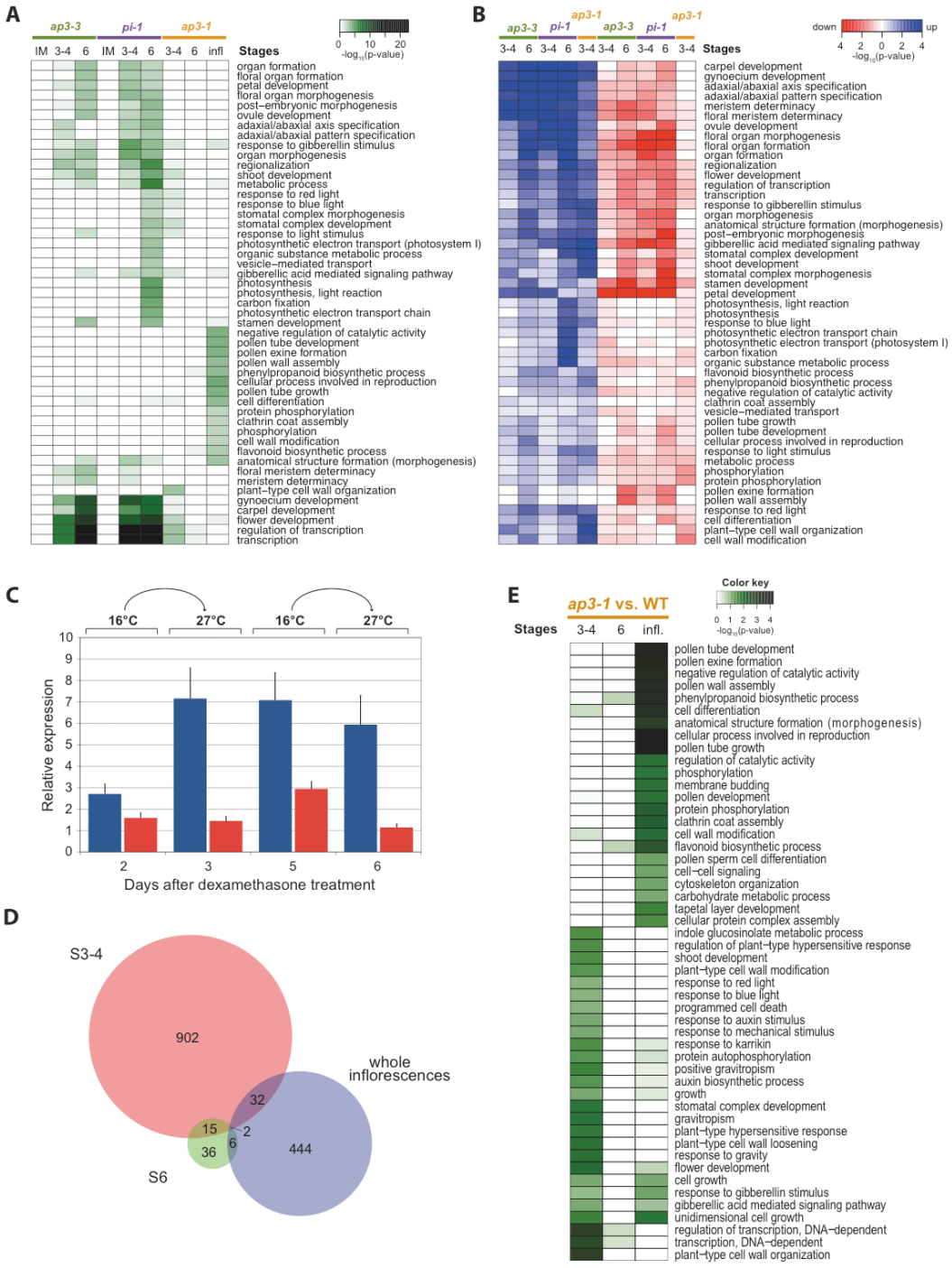

Fig. S2. Enrichment of Gene Ontology terms and directionality of gene expression changes in the microarray datasets. (A) Gene Ontology terms identified as significantly enriched (BH-adjusted *p*-value< 0.01) in the datasets stemming from the different microar-

ray experiments (as indicated). BH-adjusted *p*-values are shown. (B) Directionality of co-ordinated gene expression changes within enriched Gene Ontology terms as determined by a gene set enrichment analysis (23). Down-regulation is represented by red, up-regulation by blue color. (C) Reduction of wild-type *AP3* mRNA levels in *ap3-1* mutant flowers in the floral induction system background upon a shift from permissive to non-permissive temperatures. Relative *AP3* mRNA levels were determined by qRT-PCR in flowers collected from 35S:AP1-GR *ap1-1 cal-1* (blue bars) and 35S:AP1-GR *ap1-1 cal-1 ap3-1* (red bars) plants at different days after dexamethasone treatment (as indicated). Plants of both genotypes were grown at 16ºC followed by a shift to a non-permissive temperature (27ºC) for 24 h. Tissue was harvested directly before (at days 2 and 5 after dexamethasone treatment) and after the temperature-shift (at days 3 and 6 after dexamethasone treatment). Error bars indicate s.e.m. of four qRT-PCR experiments. The strong increase in *AP3* mRNA levels in wild-type flowers between day 2 and 3 of the experiment is a consequence of temporal expression changes of *AP3* during early flower development (9). In agreement with a previous report (14), wild-type *AP3* mRNA levels were already reduced in *ap3-1* mutant flowers at permissive temperatures when compared to the wild type, and fell further upon a shift to non-permissive temperatures. (D) Venn diagram showing the number of genes that were identified as differentially expressed in the different *ap3-1* microarray experiments (3 and 6 d time-points in the floral induction system as described for panel C, and whole inflorescences) and the overlap between the gene sets. (E) Gene Ontology terms detected as enriched (BH-adjusted *p*-value< 0.05) in the different *ap3-1* microarray experiments (as indicated). In panels A, B and E, the negative decadal logarithms of *p*-values (BH-adjusted in

panel (A)) are represented through color-coding (see color key in the upper right-hand corner of each panel). ‘IM’: infloresence-like meristem; ‘infl.’: inflorescence.

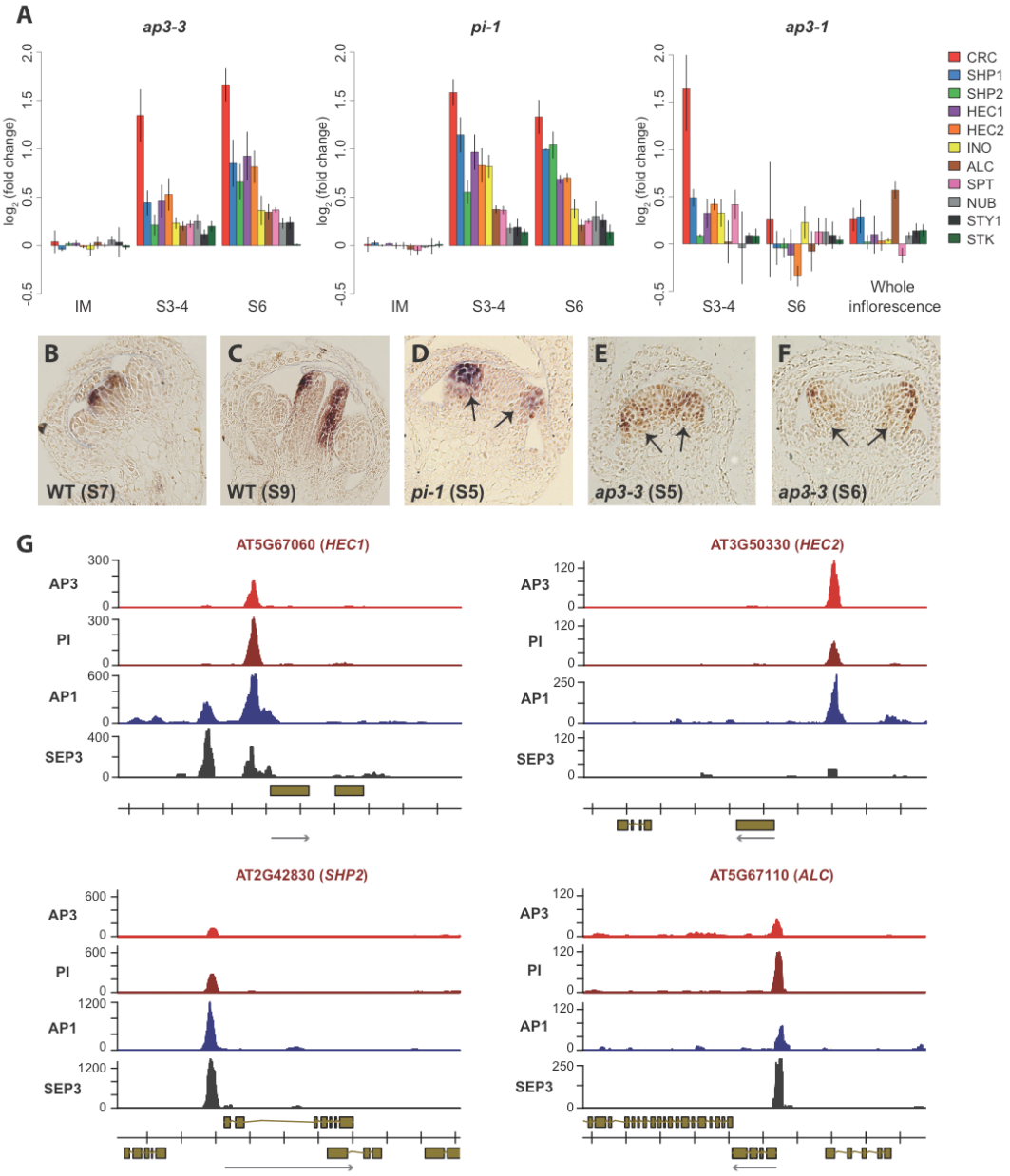

Fig. S3. AP3/PI-dependent regulation of genes involved in carpel development. (A) Transcriptional response of selected genes involved in carpel development to a perturbation of B function. Log_2-transformed fold change values from the *ap3-3*, *pi-1* and *ap3-1* microarray experiments are shown for selected genes (see Table S3 for full gene names). Error bars represent ± 1 s.e.m.. 'IM': inflorescence-like meristem. (B-F) Re-

sults of *in situ* hybridizations using a *CRC* antisense probe. Longitudinal sections of flowers of wild-type (B-C), *pi-1* (D) and *ap3-3* (E-F) flowers are shown. Approximate floral stages (S) are indicated. Arrows in panels D-F point to expression in 3rd whorl organ primordia. (G) ChIP-Seq results for selected target genes involved in carpel development (as indicated). In each plot, the two uppermost traces represent AP3 and PI data, respectively, followed by those for AP1 (11) and SEP3 (29), which are shown for comparison. Genes found in the genomic regions analyzed, their exon-intron structure, and the direction of transcription (arrows) are indicated at the bottom of each panel.

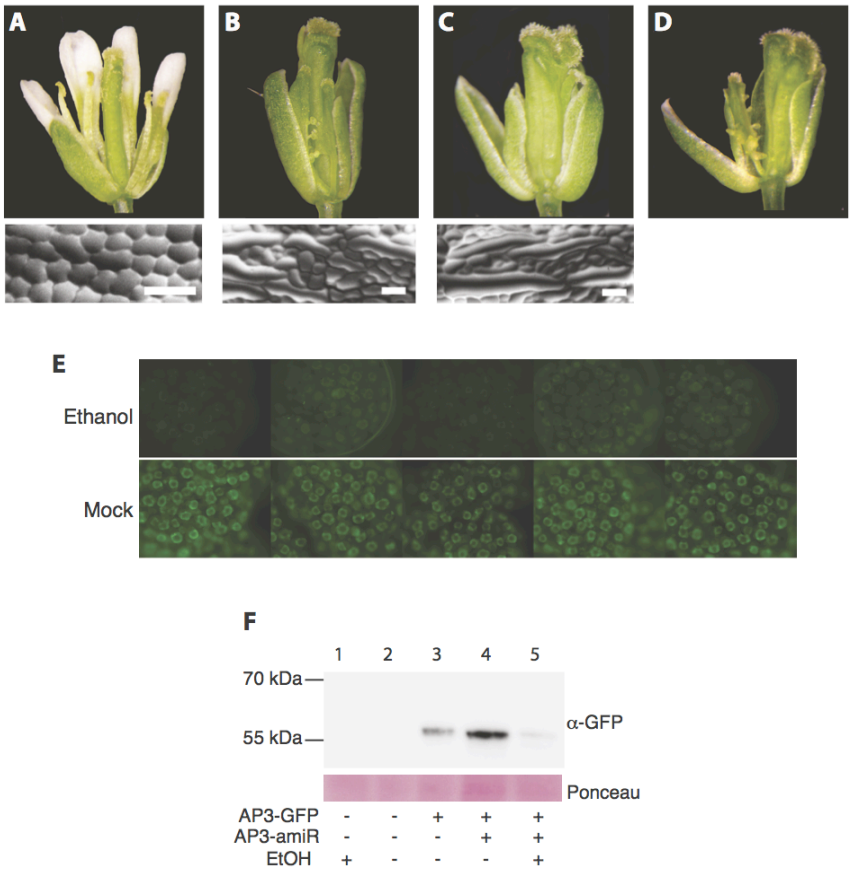

Fig. S4. Identification of amiRNAs mediating an efficient knockdown of *AP3* and *PI*. (A) A wild-type flower. (B) Flower of a plant expressing the PI-amiRNA PI(10) under control of the CaMV 35S promoter. Petals and stamens are transformed into sepals and carpels, respectively. (C) and (D) Flowers of plants expressing the AP3-amiRNAs AP3(1) (panel C) and AP3(2) (panel D) under control of the CaMV 35S promoter. Expression of both amiRNAs led to floral phenotypes resembling those of *ap3* mutant plants (Fig. 2C). The AP3(1)-amiRNA was used in the knockdown experiments described in this study. Bottom sections of panels A-C show cells in the abaxial epidermis of 2nd whorl organs. Scale bars: 40 μm. (E-F) Effect of AP3 amiRNA induc-

tion on *AP3* mRNA levels and AP3-GFP protein accumulation. (E) Fluorescence microscopy images of inflorescences of 35S:AP1-GR pAP3:AP3-GFP 35S:AlcR/pAlcA:AP3(1)-amiRNA *ap1-1 cal-1 ap3-3* plants 3 d after dexamethasone treatment. Two days after the dexamethasone treatment, the plants were either exposed to ethanol vapor for 6 h (upper section of the panel) in order to induce amiRNA expression, or were mock-treated (lower section of the panel), followed by an 18 h recovery period. All images were taken with the same microscope settings to allow a qualitative comparison of the GFP signals. (F) Immunoblot using GFP-specific antibodies and protein extracts of nuclei isolated from inflorescences of 35S:AP1-GR *ap1-1 cal-1* plants (lanes 1 and 2), 35S:AP1-GR pAP3:AP3-GFP *ap1-1 cal-1 ap3-3* plants (lane 3), and 35S:AP1-GR pAP3:AP3-GFP 35S:AlcR/pAlcA:AP3(1)-amiRNA *ap1-1 cal-1 ap3-3* plants (lanes 4 and 5), respectively. Inflorescence tissue was collected 4 d after the induction of flower formation through treatment with a dexamethasone-containing solution. Plants used for the samples analyzed in lanes 1, 4 and 5 were treated for 6 h with ethanol vapor (lanes 1 and 5), or were mock-treated (lane 4), followed by an 18 h recovery period prior to tissue collection. The approximate sizes of molecular weight markers are indicated on the left. The lower section of the panel shows part of the membrane used for the immunoblot, which was stained by Ponceau S after protein transfer to test for approximately equal loading.

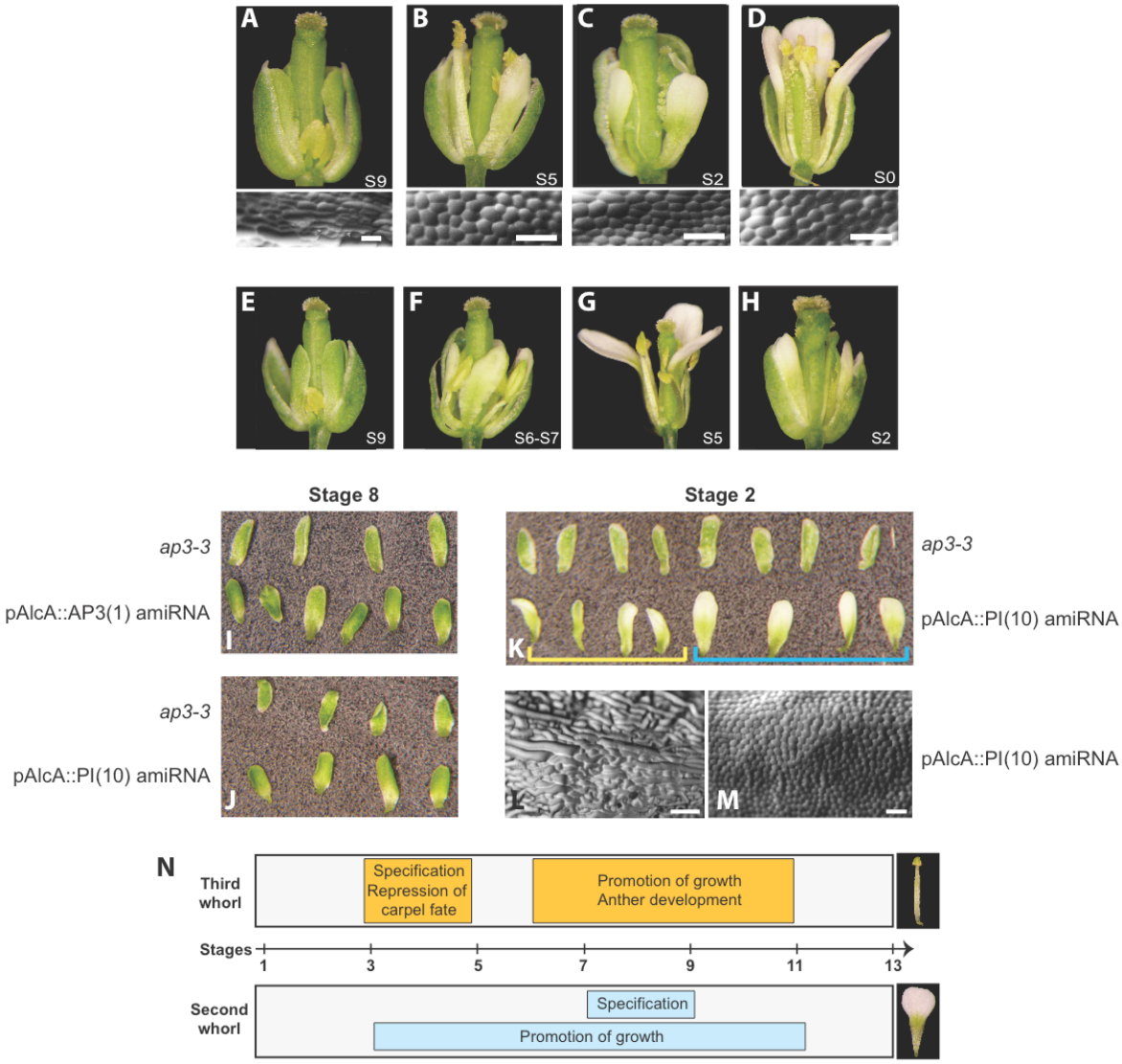

Fig. S5. Effects of *PI* and *AP3* gene perturbations on flower development. (A-D) Flowers of 35S:AlcR/ pAlcA:AP3-amiRNA plants after a single 24 h treatment with ethanol vapor. The approximate developmental stages (S) of the flowers at the time of treatment are indicated. Bottom sections of panels A-D show cells in the abaxial epidermis of 2nd whorl organs. Scale bars: 40 µm. (E-H) Flowers of a 35S:AlcR/pAlcA:PI(10)-amiRNA plant that was treated for 24 h with ethanol vapor. Flowers were photographed at time of anthesis. The approximate stages (S) of the flow-

ers at the time of *PI* perturbation are indicated. (I-K) Morphology of second whorl organs in flowers of 35S:AlcR/pAlcA:AP3(1)-amiRNA (panel I) and 35S:AlcR/pAlcA:PI(10)-amiRNA (panels J-K) plants. Plants were treated for 24 h with ethanol vapor. The approximate stages of the flowers at the time of *AP3* and *PI* perturbation are indicated. For comparison, second whorl organs of *ap3-3* mutant flowers are shown in the upper section of each panel. Second whorl organs shown in panel K were either petaloid (blue bracket) or were chimeric, exhibiting both sepal and petal characteristics (yellow bracket). (L-M) Abaxial surfaces of the chimeric (L) and the petaloid (M) second whorl organs shown in panel K. Scale bars: 40 μm. (N) Role of B function during *Arabidopsis* flower development. Graphical representation of results from the B function perturbation experiments shown in Fig. 3 and Fig. S5A-M. The approximate developmental stages during which certain functions are active in 2nd and 3rd whorl organs are indicated.

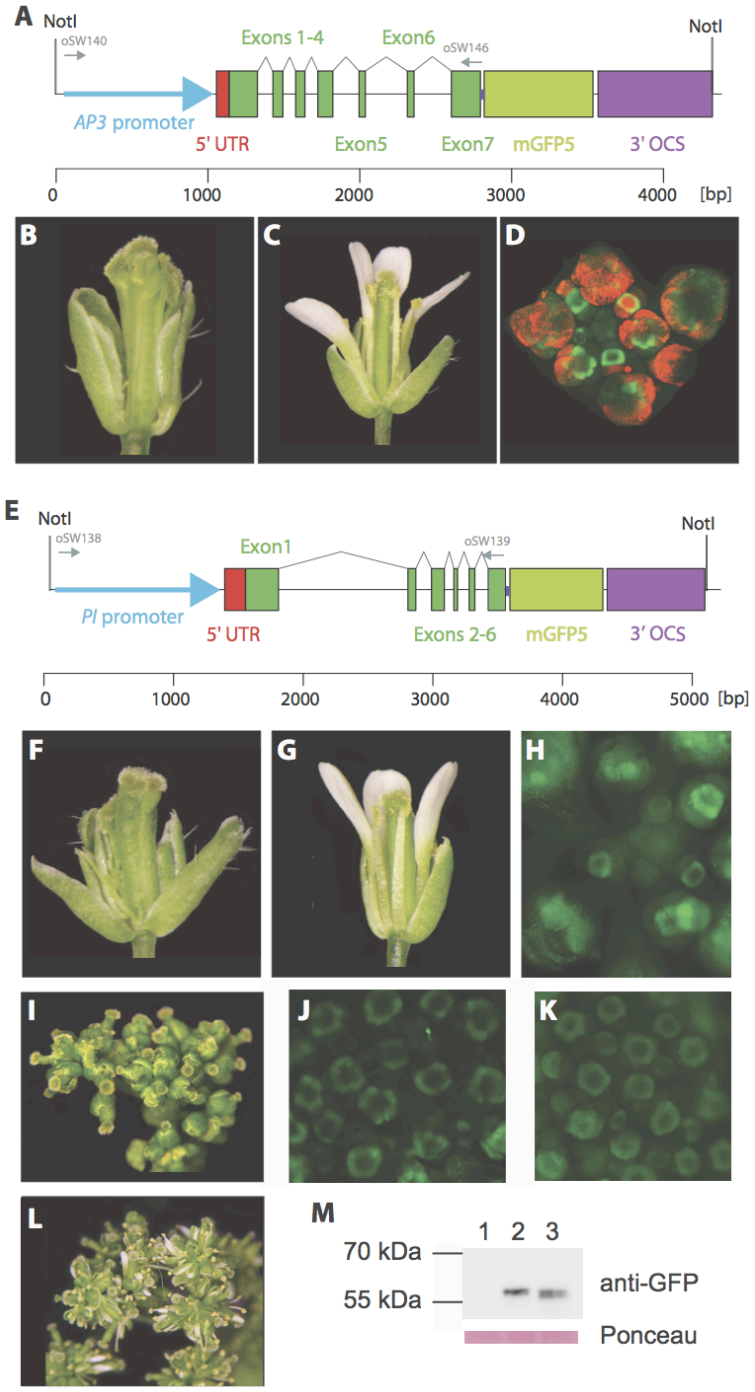

Fig. S6. Generation and characterization of AP3-GFP and PI-GFP lines. (A) Schematic representation of the construct used to express a fusion between AP3 and GFP (mGFP5) from the *AP3* promoter. The positions of primers used to PCR amplify a

genomic *AP3* fragment are indicated (oSW140 and oSW146). (B) An *ap3-3* mutant flower. (C) Flower of a pAP3:AP3-GFP *ap3-3* plant which resembles wild-type flowers. (D) Confocal microscopy image of an inflorescence of a pAP3:AP3-GFP *ap3-3* plant. (E) Schematic representation of the construct used to express a fusion between PI and GFP (mGFP5) from the *PI* promoter. The positions of primers used to PCR amplify a genomic *PI* fragment are indicated (oSW138 and oSW139). (F) A *pi-1* mutant flower. (G) Flower of a pPI:PI-GFP *pi-1* plant which resembles wild-type flowers. (H) Fluorescence microscopy image of an inflorescence of a pPI:PI-GFP *pi-1* plant. (I) Inflorescence of a 35S:AP1-GR *ap1-1 cal-1 ap3-3* plant 17 d after treatment with a dexamethasone-containing solution. Flowers lack petals and stamens. (J) Fluorescence microscopy image of an inflorescence of a 35S:AP1-GR pAP3:AP3-GFP *ap1-1 cal-1 ap3-3* plant 4 d after treatment with a dexamethasone-containing solution. (K) Fluorescence microscopy image of an inflorescence of a 35S:AP1-GR pPI:PI-GFP *ap1-1 cal-1 pi-1* plant 3 d after treatment with a dexamethasone-containing solution. (L) Inflorescence of an 35S:AP1-GR pAP3:AP3-GFP *ap1-1 cal-1 ap3-3* plant 17 d after treatment with a dexamethasone-containing solution. Flowers form petals and stamens (compare to panel I). (M) Immunoblot using GFP-specific antibodies and protein extracts from inflorescences of 35S:AP1-GR *ap1-1 cal-1* plants (lane 1), 35S:AP1-GR pAP3:AP3-GFP *ap1-1 cal-1 ap3-3* plants (lane 2), and 35S:AP1-GR pPI:PI-GFP *ap1-1 cal-1 pi-1* plants (lane 3), 4 d after treatment with a dexamethasone-containing solution. The approximate sizes of molecular weight markers are indicated on the left. The lower section of

the panel shows part of the membrane used for the immunoblot stained by Ponceau S as a loading control.

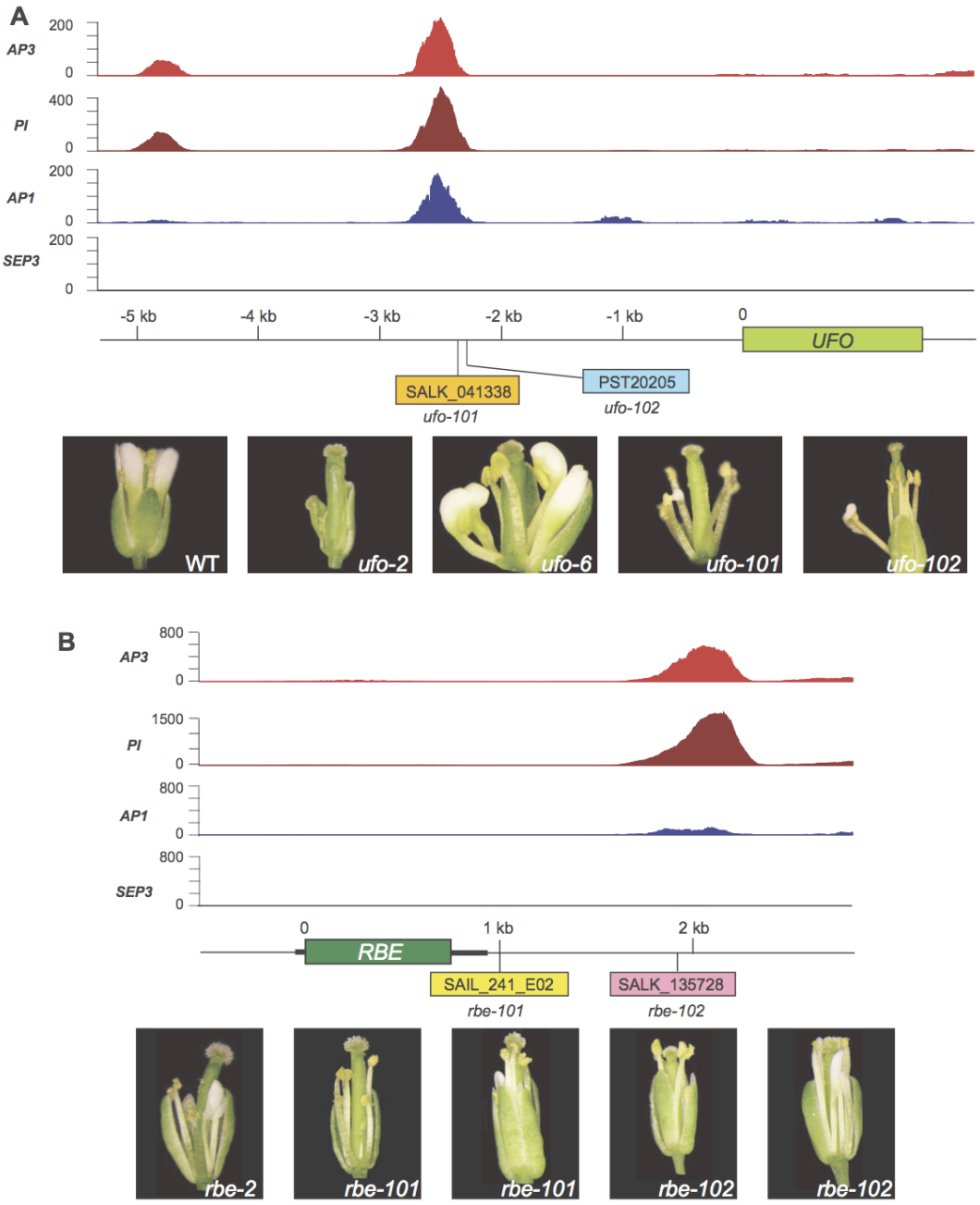

Fig. S7. Effect of T-DNA insertions in AP3/PI binding sites on gene function. (A-B) Analysis of binding sites upstream of *UNUSUAL FLORAL ORGANS* (*UFO*) (A) and downstream of *RABBIT EARS* (*RBE*) (B). The upper section of each panel shows the ChIP-Seq results for the genomic region containing the gene under study. Two uppermost traces

represent AP3 and PI data, respectively, followed by those for AP1 (11) and SEP3 (29), which are shown for comparison. The positions and identifiers of the T-DNA insertion and transposon lines we analyzed, as well as the corresponding allele names we assigned are shown. The lower section of the panels show flowers of wild type (WT) plants, of the published alleles *rbe-2*, *ufo-2* and *ufo-6*, as well as of flowers of the different T-DNA insertion lines.

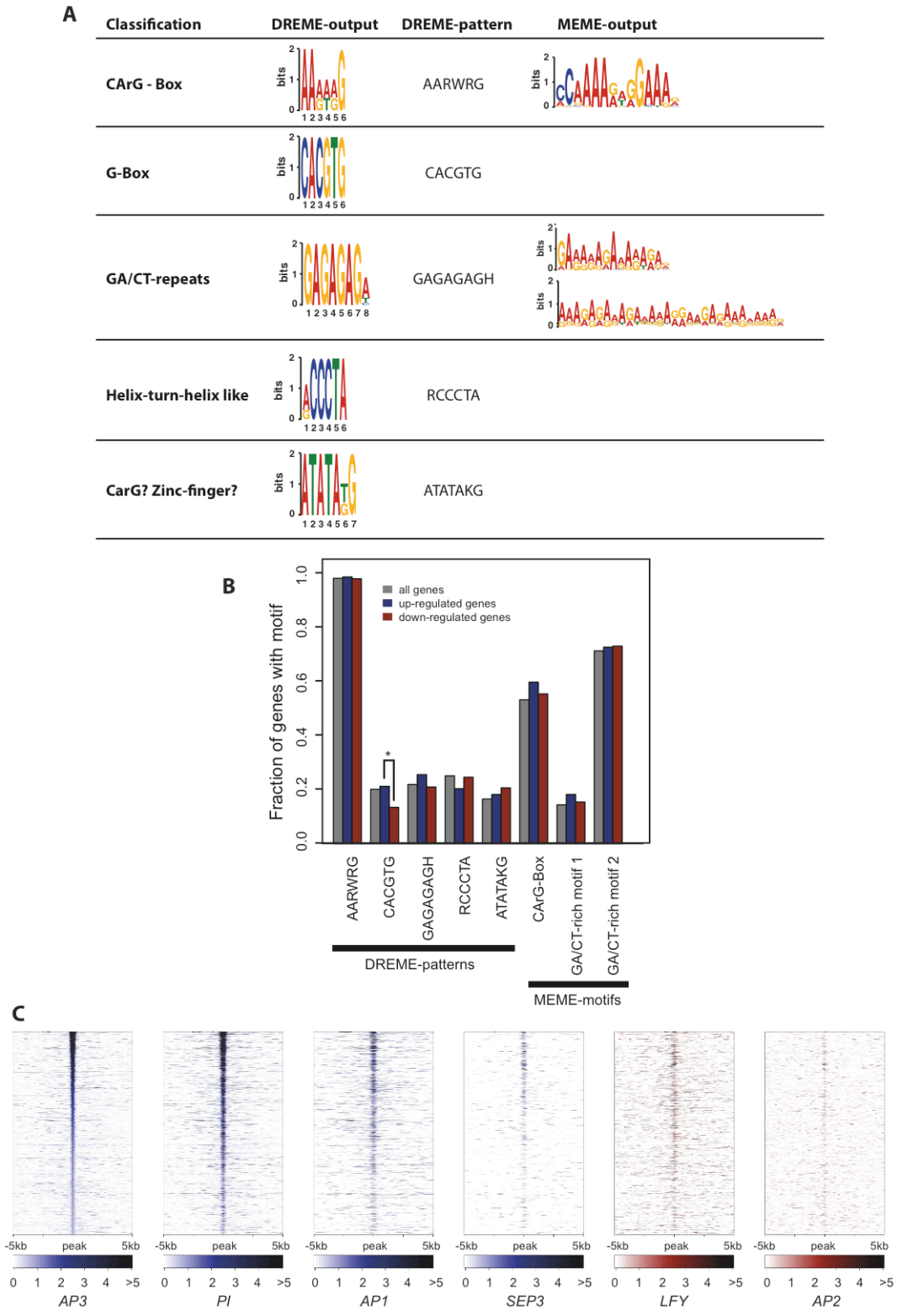

Fig. S8. Sequence motifs detected in the vicinity of AP3/PI binding sites and genome-

wide binding data for AP3/PI. (A) Results from a motif analysis performed using the MEME-Chip suite (38) using 400 bp long sequences centered around overlapping binding sites of PI and AP3. The analysis detected three significantly enriched motifs using the MEME algorithm (40) and five motifs using the DREME algorithm (39). (B) Frequency of motif occurrences within 400 bp windows of peak regions. The fraction of peaks containing a motif is shown for promoter regions of all genes in the dataset (gray bars), as well as of those in promoters of genes up (blue bars) or down-regulated (red bars) at any time point of the *pi-1* or *ap3-3* null mutant experiments. An asterisk indicates a statistically significant (Chi-square *p*-value<0.05) enrichment of G-boxes in genes repressed by AP3/PI when compared to activated genes. (C) Comparison of binding data for selected floral regulators. Heatmaps visualize the relative positions of binding sites identified in the different ChIP-Seq experiments (as indicated; data for MADS-domain proteins are shown in blue and data for LFY and AP2 in red), which are located in the vicinity of the identified AP3 peaks. Normalized Poisson enrichment scores are shown in a color code scale. All data were sorted (from top to bottom) according to descending AP3 peak height.

Table S1. amiRNAs directed against *AP3* and *PI*. Two amiRNAs against *AP3* and 10 against *PI* were designed and expressed under control of the CaMV 35S promoter in wild-type plants. The sequences of the different amiRNAs, the number of primary transformants analyzed ('No. Lines') and the observed phenotypes are indicated. Weak mutant phenotypes included male sterility due to defects in stamen elongation and pollen production, as well as petal elongation defects, resulting in small greenish petals. Strong mutant phenotypes refer to full homeotic organ transformations as observed in *ap3-3* and *pi-1* null mutants.

Name	No. Lines	No Mutant Phenotype	Weak Mutant Phenotype	Strong Mutant Phenotype	amiRNA Sequence
AP3(1)	10	-	-	10	TTCGCTCATATTGAGTGGGCC
AP3(2)	24	5	12	7	TACTAGTCCATAGTGACGGTC
PI(1)	4	4	-	-	TAGTTCGAAACGTTTAGGCAG
PI(2)	10	9	1	-	TAGTTCGAAACGTTTAGGCGC
PI(3)	9	9	-	-	TAGTTCGAAACGTTTAAGCGC
PI(4)	5	5	-	-	TGTTTAAGCACACAGCACAGC
PI(5)	7	6	1	-	TAGAACGTCACCACTCTGTTC
PI(6)	9	7	2	-	TGACAAACTAAAGACCACGGT
PI(7)	17	17	-	-	TCATGTTCAATGGCGTGCCCG
PI(8)	11	11	-	-	TGAGATTATAAAATCTCGACG
PI(9)	16	16	-	-	TGACTGTATATCTTGTCCGTT
PI(10)	4	-	-	4	TCTTTGAGAACGTCACCACTC

Table S2. Examples of high-confidence target genes of AP3/PI. Genes listed were associated with one or more binding peaks and were differentially expressed in at least one of the microarray datasets.

Function	Gene ID	Gene Name
Petal and Stamen Development	At3g54340	APETALA3
	At5g20240	PISTILLATA
	At1g30950	UNUSUAL FLORAL ORGANS

	At4g27330	SPOROCYTELESS
	At5g03680	PETAL LOSS
	At3g02000	ROXY1
	At1g08320	TGACG (TGA) MOTIF-BINDING PROTEIN 9
	At5g06839	TGACG (TGA) MOTIF-BINDING PROTEIN 10
Female Reproductive Development	At1g69180	CRABS CLAW
	At2g42830	SHATTERPROOF 2
	At5g67060	HECATE 1
	At3g50330	HECATE 2
	At5g67110	ALCATRAZ
	At5g18000	VERDANDI
Floral Organ Boundary	At3g15170	CUP-SHAPED COTYLEDON 1
	At1g76420	CUP-SHAPED COTYLEDON 3
	At3g23130	SUPERMAN
Hormone Response	At3g23030	INDOLE-3-ACETIC ACID INDUCIBLE 2
	At1g51950	INDOLE-3-ACETIC ACID INDUCIBLE 18
	At4g29080	INDOLE-3-ACETIC ACID INDUCIBLE 27
	At2g33860	ETTIN
	At1g78440	GIBBERELLIN 2-OXIDASE 1
	At4g21690	GIBBERELLIN 2-OXIDASE 3
	At1g47990	GIBBERELLIN 2-OXIDASE 4
	At1g70700	JASMONATE-ZIM-DOMAIN PROTEIN 9
	At5g13220	JASMONATE-ZIM-DOMAIN PROTEIN 10

Table S3. Genes discussed in this study. Gene identifiers, gene names and aliases are shown.

Gene ID	Gene Name	Alias
At4g18960	AGAMOUS	AG
At5g67110	ALCATRAZ	ALC
At1g69120	APETALA1	AP1
At4g36920	APETALA2	AP2
At3g54340	APETALA3	AP3
At4g39400	BRASSINOSTEROID INSENSITIVE 1	BRI1
At1g69180	CRABS CLAW	CRC
At5g53950	CUP-SHAPED COTYLEDON2	CUC2
At1g76420	CUP-SHAPED COTYLEDON3	CUC3
At5g67060	HECATE1	HEC1

At3g50330	HECATE2	HEC2
At4g29080	INDOLE-3-ACETIC ACID INDUCIBLE 27	IAA27
At1g23420	INNER NO OUTER	INO
At5g61850	LEAFY	LFY
At5g08717	MICRORNA166D	MIR166D
At4g27330	NOZZLE/SPOROCYTELESS	NZZ/SPL
At1g13400	NUBBIN	NUB
At5g20240	PISTILLATA	PI
At5g06070	RABBIT EARS	RBE
At3g17010	REPRODUCTIVE MERISTEM22	REM22
At4g09960	SEEDSTICK	STK
At1g24260	SEPALLATA3	SEP3
At3g58780	SHATTERPROOF1	SHP1
At2g42830	SHATTERPROOF2	SHP2
At4g36930	SPATULA	SPT
At3g51060	STYLISH1	STY1
At3g23130	SUPERMAN	SUP
At1g30950	UNUSUAL FLORAL ORGANS	UFO

Table S4. Primers used for PCR genotyping and generation of constructs. Names and sequences of primers are shown. If a restriction site was incorporated through use of a primer, the corresponding sequence is underlined.

Primer	**Forward Primer (5` -> 3`)**
oSW-140	ATCCCGGGATGCATAGTTGACCCTGTTTTAAGG
oSW-146	ATCCCGGGTACCTGGTCCTTCAAGAAGATGGAAGGTAATGATGTC
oSW-138	ATCTGCAGGAGGCTAAACAAGTAAACATGACCTG
oSW-139	ATCTCGAGGGACCATCGATGACCAAAGACATAATCTTTTCC
oSW-721	GTCTTTCATGTGCCAACCACTG
oSW-722	GAAGAGGGCAAAGACGGATGTG
oSW-717	AGCCTATAATTGGGTGGTGAC
oSW-718	CAGAAGCCGAATTTCCTAAAGAGG
KH141	TTCTAACTAATTTGTCCGCGC
KH144	TACCTCGGGTTCGAAATCGAT
KH171	GGAAAATAAAACTAGCTTTCATACAAATCTCAAATATAT
oSW-689	ATAAATACAAGCCTCCTAACTCA
oSW-690	CGGTTGTATGCAGATGGGAG
SAIL_LB	GCCTTTTCAGAAATGGATAAATAGCCTTGCTTCC
SALK_LB	CTTTGACGTTGGAGTCCAC
SALK_LB2	CCAAACTGGAACAACACTCAACCCTATCTC

Table S5. Primers used for qRT-PCR analysis. Gene identifiers, gene aliases and primer sequences are shown.

Gene ID	Alias	Forward primer (5` -> 3')	Reverse primer (5` -> 3')
At3g54340	AP3[a]	TCCGGACTCAGATCAAGCA	TTCCATTTCATCCTCAAGACG
At3g54340	AP3[b]	AGCTGGAACTAAGAGCTGAAGATCCTC	ACGTGACCCTTCGATTTGGTATCCAAG
At5g20240	PI	ACAAAGTCCGAGACCACCAGATG	CCTCTTGCGTTGCTTGCTATAGC
At3g23130	SUP	GAGGCTGGAGAGGCTACAAG	AATTAAGCGAAACCCAAACGGAG
At3g17010	REM22	CGAGAAACAAAGTGAAGAAGAAGAGC	TTGGTATTGCCAGGAACTTGAGG
At1g69180	CRC	CCAACGCATCAAAAGTGCCAATCC	TTCTCACCGAATCCCAAGCCATG
At3g58780	SHP1	TACCTGCGAGCAAAGATAGCCGAAG	ACTGTCGTCCCTTGTATCACACTCG
At4g27330	SPL	AAATCATACGGGACCAATGGAGG	CAATCACCTACGAGTGACGACG
At1g30950	UFO	GGATCAAGATTCAAGCTCCGATGAGG	CTGAGGCATCCGTTCGATCTCG
At5g06070	RBE	AGGGCAAAGACGGATGTGTCAAG	GCCTTAGCTCAAGATCCAACTCCTC
At5g53950	CUC2	GCTCCAAGGATGAATGGGTGATCTC	ACAGTTGCTCCTCCTCCTCCTC
At4g34270	REF2	ATCTGCGAAAGGGTATCCAGTTGAC	TGGAAGCCTCTGACTGATGGAGC
At2g28390	REF3	CACTCTTCTATGTTGGGTCACACCAG	TTATCGCCATCGCCTTGTCTGC

a: primer sequences used to assay total *AP3* mRNA levels.
b: primer sequences used to assay wild-type only *AP3* mRNA levels (*i.e.* to exclude the *ap3-1* mRNA variant).

Table S6. Primers used for ChIP-qPCR analysis. Gene identifiers, gene aliases and primer sequences are shown.

Gene ID	Alias	Forward primer (5` -> 3')	Reverse primer (5` -> 3')
At5g06070	RBE	CAGAAGCCGAATTTCCTAAAGAGG	TCTGCAACTGCAAGAGAACTTAAC
At5g20240	PI	TAGAGTTGGCTATGTGTAATAAGCG	GCTACTTTCTTGAGGGCACAGTC
At1g69180	CRC	CGAGCATGGAAACCTGACTAAACCC	GACTGTGAGAGATGGGACGATTGC
At1g76420	CUC3	ACACATCTTCCACCGCAAGC	TTGCTATCTTTGTTCTTCCTTCTGG
At3g50330	HEC2	CCAAGTCCAAAGCAACTTACTG	AATTATTATGAGTTCGTCTTCTACCC
At5g08717	miR166D	TCTTGACCCTTTCTCTTCAGTCAC	TACAGAACCAAGTCTCAGAGGTC
At5g67110	ALC	TCTCTCTGCTCTACTCTGTGTG	GCTTCTCTGAAGAACGTGATCTC
At5g67060	HEC1	CGTTATGCCTTCTTTGCCTTTAGTG	TTTATCGCATTTATCGACCGTCCAG
At4g29080	IAA27	CCATAGGCTCTCATTTTTTGGGTC	ATTGCTACTGCGGCTAAGTGG
At3g54340	AP3	GATTTGGTGGAGAGGACAAG	GATTTAAACAGTGTCTTGTAATTA
At4g18960	AG	TCCATCGAGAAGGTTGAGAGTTCAGAC	TGTCCGAGTAACATCACAACGTTCC
At2g42830	SHP2	ACGACGAACACTCATATAAACCACCC	GGGCTCTGTTTCTCATCAGAATCACC
At3g23130	SUP	AAATGGGAGAAAGGAACATCCAC	AGGAAAGAGTGATGGGTGAATATG
At1g30950	UFO	GCGAAGCCTCTTGAGTTACTGCAA	GAGAATATCTGAAGCTGACAAGTCGCAA
At4g27330	SPL	TGCCTGCCTAAACCCAGCAATATAAATC	GGTCATTGGGCGGCTACTACTAGG
At4g26930	REF1	TCTCCGACCTTTCTTCACACCCATTCC	GTCTCCGCTTAGGAGCACGAAAGCTATC

At4g39400	BRI1	ACCCAGCACTAAACAGAAGATCAG	CCCAACCACCTATCTCTTGATTCTC
At5g09810	ACTIN	CGTTTCGCTTTCCTTAGTGTTAGCT	AGCGAACGGATCTAGAGACTCACCTTG
At4g03870	Mu	GATTTACAAGGAATCTGTTGGTGGT	CATAACATAGGTTTAGAGCATCTG C

Dataset S1. Genes identified as differentially expressed in the microarray experiments. Genes identified as differentially expressed in the *ap3-3*, *pi-1* and *ap3-1* experiments are listed in separate spreadsheets. Gene identifiers, gene aliases and gene descriptions; log_2-transformed fold-change values, *p*-values, and BH-adjusted *p*-values; and mean log_2-transformed expression values are shown for the different time-points/samples. Putative direct targets are indicated by the maximum ChIP-Seq enrichment scores of peaks in the region spanning 3 kb upstream and 1 kb downstream of a given gene. The column 'In Mara and Irish?' indicates whether or not a gene was identified as differentially expressed by Mara and Irish (42) after AP3-GR activation in *ap3-3* 35S:PI inflorescences.

Supplementary file: DatasetS1

Dataset S2. Genomic regions identified as enriched in the PI and AP3 ChIP-Seq experiments. A total of 1,852 and 1,524 genomic regions were identified as significantly enriched (CSAR False Discovery Rate<0.001 and confirmed by at least 1 bp overlap with significant regions determined by the MACS peak finder using default parameters) for PI (spreadsheet 1) and AP3 (spreadsheet 2), respectively. Chromosome numbers and genomic coordinates (start and end of peaks, according to the TAIR genome release 10), as well as the widths of the identified peaks are listed. In addition, the genomic coordinates for the nucleotide positions with the highest enrichment scores within a given region ('peak

position'), as well as the enrichment scores (based on a Poisson-distribution, calculated using the CSAR package) at these nucleotide positions are given. Putative target genes of PI and AP3 are listed in spreadsheets 3 and 4, respectively. The position of significantly enriched region(s) with respect to the corresponding gene is indicated by dividing the gene region into different segments (as indicated) and the maximum peak scores within these segments are shown. A value of 0 indicates that no significantly enriched peak region was detected within a given segment. The column 'In Mara and Irish?' indicates whether or not a gene was identified as differentially expressed by Mara and Irish (42) after AP3-GR activation in *ap3-3* 35S:PI inflorescences.

Supplementary file: DatasetS2

Dataset S3. Results of GO term, gene family/protein motif, and ROAST analyses. GO terms and protein/gene families identified as enriched or under-represented among differentially expressed genes identified in the different microarray experiments (as indicated) are shown in spreadsheets 1 and 2, respectively. The total number of genes represented on the Agilent microarray that were assigned to a specific GO term is indicated. Spreadsheet 3 lists the results from a test for coordinated changes of gene expression among sets of genes associated with significantly enriched GO terms. *P*-values for up and down-regulation are shown for the different experiments (genotypes) and time-points/samples.

Supplementary file: DatasetS3

Dataset S4. Over-represented GO terms identified among PI targets and genes identified as differentially expressed after B function perturbation. GO terms identified as significantly (BH-adjusted *p*-value< 0.01) enriched in the list of putative direct PI targets (Dataset S2) and in the list of differentially expressed genes (DEGs) from the combined set of *ap3-3* and *pi-1* microarray experiments at ~stage 6-7 (5 d time-point) are shown. For each GO term, the number of expected and observed genes in a dataset, as well as the BH-adjusted *p*-value (Fisher's Exact Test) are shown.

Supplementary file: DatasetS4

SUPPLEMENTARY REFERENCES

1. Schwab R, Ossowski S, Riester M, Warthmann N, & Weigel D (2006) Highly specific gene silencing by artificial microRNAs in Arabidopsis. *Plant Cell* 18(5):1121-1133.
2. Eshed Y, Baum SF, Perea JV, & Bowman JL (2001) Establishment of polarity in lateral organs of plants. *Curr Biol* 11(16):1251-1260.
3. Benfey PN & Chua NH (1990) The Cauliflower Mosaic Virus 35S Promoter: Combinatorial Regulation of Transcription in Plants. *Science* 250(4983):959-966.
4. Caddick MX*, et al.* (1998) An ethanol inducible gene switch for plants used to manipulate carbon metabolism. *Nat Biotechnol* 16(2):177-180.
5. Roslan HA*, et al.* (2001) Characterization of the ethanol-inducible alc gene-expression system in Arabidopsis thaliana. *Plant J* 28(2):225-235.
6. Wellmer F, Alves-Ferreira M, Dubois A, Riechmann JL, & Meyerowitz EM (2006) Genome-wide analysis of gene expression during early Arabidopsis flower development. *PLoS Genet* 2(7):e117.
7. McBride KE & Summerfelt KR (1990) Improved binary vectors for Agrobacterium-mediated plant transformation. *Plant Mol Biol* 14(2):269-276.
8. Clough SJ & Bent AF (1998) Floral dip: a simplified method for Agrobacterium-mediated transformation of Arabidopsis thaliana. *Plant J* 16(6):735-743.
9. Wellmer F, Alves-Ferreira M, Dubois A, Riechmann JL, & Meyerowitz EM (2006) Genome-Wide Analysis of Gene Expression during Early Arabidopsis Flower Development. *PLoS Genetics* 2(7):e117.
10. Horiguchi G, Fujikura U, Ferjani A, Ishikawa N, & Tsukaya H (2006) Large-scale histological analysis of leaf mutants using two simple leaf observation methods: identification of novel genetic pathways governing the size and shape of leaves. *Plant J* 48(4):638-644.
11. Kaufmann K*, et al.* (2010) Orchestration of floral initiation by APETALA1. *Science* 328(5974):85-89.
12. Edwards K, Johnstone C, & Thompson C (1991) A simple and rapid method for the preparation of plant genomic DNA for PCR analysis. *Nucleic Acids Res* 19(6):1349.
13. Riechmann JL & Meyerowitz EM (1997) Determination of floral organ identity by Arabidopsis MADS domain homeotic proteins AP1, AP3, PI, and AG is independent of their DNA-binding specificity. *Mol Biol Cell* 8(7):1243-1259.
14. Sablowski RW & Meyerowitz EM (1998) Temperature-sensitive splicing in the floral homeotic mutant apetala3-1. *Plant Cell* 10(9):1453-1463.
15. Lamb RS & Irish VF (2003) Functional divergence within the APETALA3/PISTILLATA floral homeotic gene lineages. *Proc Natl Acad Sci USA* 100(11):6558-6563.
16. Long JA & Barton MK (1998) The development of apical embryonic pattern in Arabidopsis. *Development* 125(16):3027-3035.
17. Silver JD, Ritchie ME, & Smyth GK (2009) Microarray background correction: maximum likelihood estimation for the normal-exponential convolution. *Biostatistics* 10(2):352-363.
18. Ritchie ME*, et al.* (2007) A comparison of background correction methods for two-colour microarrays. *Bioinformatics* 23(20):2700-2707.
19. Smyth GK & Speed T (2003) Normalization of cDNA microarray data. *Methods* 31(4):265-273.
20. Romanel EA, Schrago CG, Counago RM, Russo CA, & Alves-Ferreira M (2009) Evolution of the B3 DNA binding superfamily: new insights into REM family gene diversification. *PLoS One* 4(6):e5791.
21. Smyth GK (2004) Linear models and empirical bayes methods for assessing differential expression in microarray experiments. *Stat Appl Genet Mol Biol* 3:Article3.
22. Benjamini Y & Hochberg Y (1995) Controlling the False Discovery Rate - a Practical and Powerful Approach to Multiple Testing. *J Roy Stat Soc B Met* 57(1):289-300.
23. Wu D*, et al.* (2010) ROAST: rotation gene set tests for complex microarray experiments. *Bioinformatics* 26(17):2176-2182.
24. Altschul SF, Gish W, Miller W, Myers EW, & Lipman DJ (1990) Basic local alignment search tool. *J Mol Biol* 215(3):403-410.

25. Livak KJ & Schmittgen TD (2001) Analysis of relative gene expression data using real-time quantitative PCR and the 2(-Delta Delta C(T)) Method. *Methods* 25(4):402-408.
26. Czechowski T, Stitt M, Altmann T, Udvardi MK, & Scheible WR (2005) Genome-wide identification and testing of superior reference genes for transcript normalization in Arabidopsis. *Plant Physiol* 139(1):5-17.
27. Gomez-Mena C, de Folter S, Costa MM, Angenent GC, & Sablowski R (2005) Transcriptional program controlled by the floral homeotic gene AGAMOUS during early organogenesis. *Development* 132(3):429-438.
28. Kaufmann K*, et al.* (2010) Chromatin immunoprecipitation (ChIP) of plant transcription factors followed by sequencing (ChIP-SEQ) or hybridization to whole genome arrays (ChIP-CHIP). *Nat Protoc* 5(3):457-472.
29. Kaufmann K*, et al.* (2009) Target genes of the MADS transcription factor SEPALLATA3: integration of developmental and hormonal pathways in the Arabidopsis flower. *PLoS Biol* 7(4):e1000090.
30. Moyroud E*, et al.* (2011) Prediction of regulatory interactions from genome sequences using a biophysical model for the Arabidopsis LEAFY transcription factor. *Plant Cell* 23(4):1293-1306.
31. Yant L*, et al.* (2010) Orchestration of the floral transition and floral development in Arabidopsis by the bifunctional transcription factor APETALA2. *Plant Cell* 22(7):2156-2170.
32. Li RQ*, et al.* (2009) SOAP2: an improved ultrafast tool for short read alignment. *Bioinformatics* 25(15):1966-1967.
33. Muino JM, Kaufmann K, van Ham RC, Angenent GC, & Krajewski P (2011) ChIP-seq Analysis in R (CSAR): An R package for the statistical detection of protein-bound genomic regions. *Plant Methods* 7:11.
34. Durinck S, Bullard J, Spellman PT, & Dudoit S (2009) GenomeGraphs: integrated genomic data visualization with R. *BMC Bioinformatics* 10:2.
35. Li H & Durbin R (2009) Fast and accurate short read alignment with Burrows-Wheeler transform. *Bioinformatics* 25(14):1754-1760.
36. Li H*, et al.* (2009) The Sequence Alignment/Map format and SAMtools. *Bioinformatics* 25(16):2078-2079.
37. Zhang Y*, et al.* (2008) Model-based analysis of ChIP-Seq (MACS). *Genome Biol* 9(9):R137.
38. Bailey TL*, et al.* (2009) MEME SUITE: tools for motif discovery and searching. *Nucleic Acids Res* 37(Web Server issue):W202-208.
39. Bailey TL (2011) DREME: motif discovery in transcription factor ChIP-seq data. *Bioinformatics* 27(12):1653-1659.
40. Bailey TL & Elkan C (1994) Fitting a mixture model by expectation maximization to discover motifs in biopolymers. *Proceedings of the Second International Conference on Intelligent Systems for Molecular Biology*, (AAAI Press), pp 28-36.
41. Chae E, Tan QK, Hill TA, & Irish VF (2008) An Arabidopsis F-box protein acts as a transcriptional co-factor to regulate floral development. *Development* 135(7):1235-1245.
42. Mara CD & Irish VF (2008) Two GATA transcription factors are downstream effectors of floral homeotic gene action in Arabidopsis. *Plant Physiol* 147(2):707-718.